Li Jian (Orcid ID: 0000-0002-7378-8658)

Discovery of rosin-based acylhydrazone derivatives as potential antifungal agents against rice *Rhizoctonia solani* for sustainable crop protection

Running title: Rosin-derived fungicides

Renle Xu,[a] Shihao Gu,[a] Kun Chen,[a] Jinyu Chen,[a] Yong Wang,[b] Yanqing Gao,[b] Shibin Shang,[c] Zhanqian Song, [c] Jie Song,[d] and Jian Li[a]*

[a] *College of Forestry, Northwest A&F University, Yangling, Shaanxi 712100, People's Republic of China*

[b] *College of Plant Protection, Northwest A&F University, Yangling, Shaanxi 712100, People's Republic of China*

[c] *Institute of Chemical Industry of Forest Products, Chinese Academy of Forestry, Nanjing, Jiangsu 210042, People's Republic of China*

[d] *Department of Chemistry and Biochemistry, University of Michigan-Flint, Flint, Michigan 48502, United States*

* *Corresponding to: Jian Li, College of Forestry, Northwest A&F University, Yangling, Shaanxi 712100, People's Republic of China. E-mail: ericlee99@nwsuaf.edu.cn*

Abstract

BACKGROUND: The use of fungicides to protect crops from diseases is an effective method, and the novel environmental-friendly plant-derived fungicides with enhanced performance and low toxicity are urgent requirements for sustainable agriculture.

RESULTS: Two kinds of rosin-based acylhydrazone compounds were designed and prepared. Based on the antifungal activity assessment against *Rhizoctonia solani*, *Fusarium oxysporum*, *Phytophthora capsici, Sclerotinia sclerotiorum*, and *Botrytis cinerea*, acylhydrazone derivatives containing thiophene ring were screened, and they showed an inhibitory effect on rice *R. solani*. Among these, Compound **4n**, with an electron-withdrawing group on the benzene ring structure attached to the thiophene ring, showed optimal activity, and the EC_{50} value was 0.981 mg/L, which was lower than that of carbendazim. Furthermore, it was indicated that **4n** could affect the mycelial morphology, cell membrane permeability and microstructure, cause the generation of ROS in fungal cells and damage the nucleus and mitochondrial physiological function, resulting in the cell death of *R. solani*. Meanwhile, Compound **4n** exhibited a better therapeutic effect on *in vivo* rice plants. However, the induction activity of **4n** on the defense enzyme in rice leaf sheaths showed that **4n** stimulates the initial resistance of rice plants by removing active oxygen, thereby protecting the cell membrane or enhancing the strength of the cell wall. Through the quantitative structure-activity relationship study, the quantitative chemical and electrostatic descriptors significantly affect the binding of **4n** with the receptor, which improves its antifungal activity.

CONCLUSION: This study provides a basis for exploiting potential rosin-based fungicides in promoting sustainable crop protection.

Keywords: rosin; acylhydrazone; thiophene ring; antifungal activity; *R. solani*; action

mechanism

1 INTRODUCTION

Plant disease is a natural disaster that severely endangers the production of agricultural crops.[1, 2] According to studies, more than 10,000 plant diseases caused by pathogenic fungi account for 10-30% of the total annual crop loss.[3, 4] For example, rice *Rhizoctonia solani* can cause premature death of rice leaf sheaths and leaves, affect grain filling, form a large number of blighted grains, and even cause the whole rice plant to rot and die, seriously affecting rice yield.[5, 6] The use of chemical fungicides to protect crops from diseases is an effective method of meeting the growing demand of humans for food.[7, 8] However, with the wide application of fungicides, many pathogens have developed strong resistance to existing fungicides, and the residues of fungicides have caused serious harm to food safety and the ecological environment.[9] Based on the above, novel fungicides with enhanced performance, low toxicity, and less residue are urgently required for sustainable agriculture.[10] Natural products and their derivatives have unique biocompatibility, novel structural skeletons and broad biological activities and are still an important fountainhead of developing pesticides today.[11]

Rosin, a valuable natural renewable plant resource, is mainly composed of resinolic acids.[12] Rosin has the advantages of extensive biological activity and good environmental compatibility in the field of agricultural production. Since it is difficult to produce resistance from rosin, it is additionally a suitable precursor for the development of efficient botanical fungicides.[13, 14] However, like other botanical pesticides, rosin has the disadvantages of slow efficacy and unstable active ingredients. In the development of rosin-based fungicides, the structural modification and optimization is necessary to improve its biological activity.[15, 16]

The acylhydrazone molecule contains two active substructure groups of amide

and Schiff base (-CONHN=CH-), and performs excellent biological and coordination abilities in a biophilic environment.[17] As an important pesticide for crop protection, acylhydrazone compounds exhibit excellent insecticidal, antifungal, and herbicidal activities.[15, 18] For instance, commercialized fungicides containing acylhydrazone groups, like Benquinox (Figure S1), exert fungicidal activity against Pythium and various diseases on rice.[19-22] Thiophene, as a sulfur-containing five-membered heterocyclic compound, plays a critical role in many biochemical processes, such as improving pharmacokinetic properties and reducing the pesticidal toxicity and side effect.[23] In recent years, antifungal compounds containing thiophene structures have also been reported to be frequently used in the design and synthesis of pesticides.[24, 25]

Based on the advantages of pine-derived botanical fungicides, two series of rosin-based acylhydrazone fungicides were designed and prepared based on principles of bioelectronic isosterization and splicing using rosin as a precursor. To enhance the activity, the thiophene group was introduced into a series of compounds. Moreover, the action mechanism of rosin-based acylhydrazone fungicides on *Rhizoctonia solani* (*R. solani*) was investigated by assessing the physicochemical properties related to antifungal activity and computational chemistry. Thus, rosin-based acylhydrazone fungicides with novel structures can be identified, which would enrich the synthesis and design of efficient botanical fungicides and broaden the application scope of pine resin.

2 MATERIALS AND METHODS

2.1 Materials and instruments

The reagents and structural characterization instruments can be seen in the Supporting Information.

2.2 Preparation for dehydroabietyl acylhydrazone compounds (3a-3p and 4a-4p)

Referring to previous methods, dehydroabietic acid (**1**) was prepared from rosin.[14] Then, 3.00 g (10 mmol) Compound **1** and 20 mmol sulfoxide chloride were refluxed in 80 mL dichloromethane for 4 h. The solvent and excess sulfoxide chloride were evaporated under vacuum to obtain compound dehydroabietyl chloride. Without posttreatment, dehydroabietyl chloride was solubilized in 50 mL tetrahydrofuran (THF) and then added dropwise to 2 mL hydrazine hydrate (80%) at room temperature. Subsequently, dehydroabietyl acylhydrazide (**2**) was obtained by recrystallization with ethanol. Compound **2** (3.14 g, 10 mmol) and 10 mmol substituted benzaldehyde or thiophene-2-formaldehyde were solubilized in 200 mL absolute ethanol and subjected to heating reflux, while thin layer chromatography (TLC) was used to track the reaction process. Dehydroabietyl acylhydrazone (**3a-3p** and **4a-4p**) was prepared by recrystallization through anhydrous ethanol (**Scheme 1**).

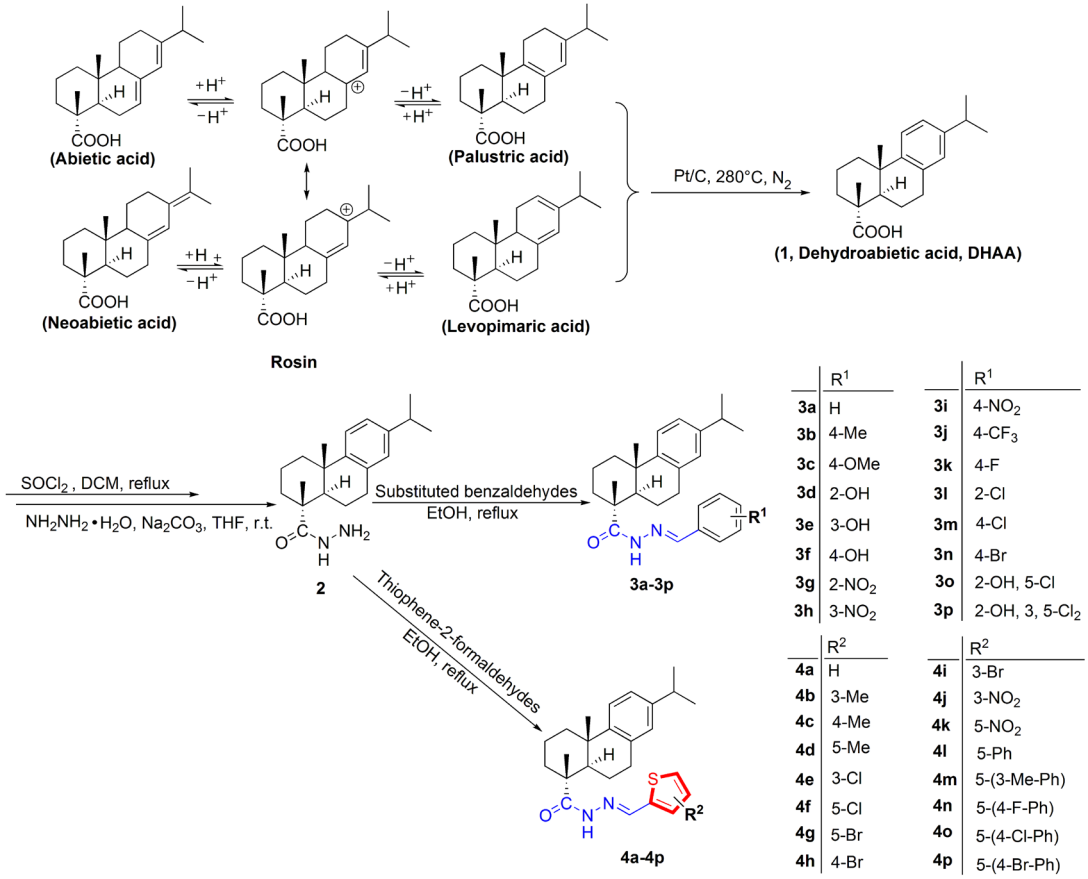

Scheme 1. Synthetic routes of rosin-based acylhydrazones (**3a-3p** and **4a-4p**)

2.3 Antifungal activity *in vitro*

The *in vitro* inhibitory activities of the dehydroabietyl acylhydrazone compounds against five plant pathogenic fungi, including *R. solani*, *Fusarium oxysporum (F. oxysporum), Phytophthora capsici (P. capsici)*, *Sclerotinia sclerotiorum (S. sclerotiorum)*, and *Botrytis cinerea (B. cinerea)*, were determined by the mycelial growth rate method in the Supporting Information.[26]

2.4 Effect of dehydroabietyl acylhydrazone (4n) on cell membrane permeability of *R. solani*

The conductivity method in the Supporting Information was used to determine the increase of cell membrane permeability caused by Compound **4n**.[14]

2.5 Antifungal activity *in vivo*

Compound **4n** and the positive control carbendazim were further tested in an indoor pot experiment against *R. solani* in the Supporting Information.[27]

2.6 Effect of dehydroabietyl acylhydrazone (4n) on defense enzyme induction activity in rice leaf sheaths

All rice plant leaf sheaths at a similar growth stage were sprayed with water and Compound **4n** at 500 mg/L until runoff and maintained at 25 °C with 80% humidity. The rice leaf sheaths were inoculated *in vivo*. After incubation for 1, 2, 3, 5, and 7 d, the levels of superoxide dismutase (SOD), catalase (CAT), phenylalanine ammonia lyase (PAL), and polyphenol oxidase (PPO) were determined using commercial kits according to the manufacturer's instructions (Nanjing Jiancheng Bioengineering Institute, Nanjing, China).

2.7 The influence of dehydroabietyl acylhydrazone (4n) on the mycelial morphology and microstructure of *R. solani*

According to the reported method, the drug-containing medium with Compound

4n (EC_{50} value of 0.981 mg/L) and the blank control (DMSO) were first prepared, and then inoculated with the *R. solani* which activated in the potato dextrose agar (PDA) medium, and cultured at 25 °C for 3 days. Finally, the hyphal samples were pretreated separately, and the effect of Compound **4n** on hyphal morphology and microstructure was observed by scanning electron microscopy (SEM, S-3400N, Hitachi, Ltd., Tokyo, Japan) and transmission electron microscopy (TEM, JEM-1230, JEOL, Ltd., Tokyo, Japan).[14]

2.8 Confocal laser scanning microscope determination of *R. solani*

According to our previously reported method, the activated *R. solani* were prepared into a 5 mm diameter mycelial disk, and incubated in potato dextrose broth (PDB) at 25 °C for 4 days. Then, the Compound **4n** (EC_{50} value of 0.981 mg/L) was added and cultured for 2 days. The blank control was treated with DMSO. Finally, after staining with 2', 7'-dichlorodihydrofluorescein diacetate (DCFH-DA), Hoechst 33258 and Rhodamine 123, respectively, the reactive oxygen species (ROS), nuclear morphology and mitochondrial membrane potential (MMP) of *R. solani* were determined by a confocal laser scanning microscope FV3000 (Olympus, Co., Tokyo, Japan).[28]

2.9 Quantitative structure-activity relationship (QSAR) analysis

According to our previously reported method, the structures of dehydroabietyl acylhydrazone derivatives (**3a**-**3p** and **4a**-**4p**) were optimized according to the density functional theory (DFT) in Gaussian software (Gaussian, Inc., Wallingford, USA), and then the linear regression relationship model of the compounds and the antifungal activity against *R. solani* was established by Codessa software (Semichem, Inc., Shawnee, USA), and the model is verified by internal test and "leave-one-out" method. Meanwhile, the structural descriptors that affect the antifungal activity against *R.*

solani were screened.[14]

3 RESULTS AND DISCUSSION

3.1 The synthesis of dehydroabietyl acylhydrazone compounds (3a-3p and 4a-4p)

Acylhydrazone is a specific kind of Schiff base. The classical method was used to synthesize dehydroabietyl acylhydrazone (**Scheme 1**).[17] First, the rosin-based hydrazide intermediate was obtained by the reaction between dehydroabietic acid and hydrazine hydrate. Then, the target product was prepared by nucleophilic addition and dehydration elimination reaction between the intermediate and the corresponding aldehyde/ketone. Subsequently, the rosin-based acylhydrazone compounds included amide bonds, imine groups, and thiophene groups were synthesized (**4a-4p**). Since the *p-π* conjugate was formed by the lone pair of electrons on the N atom in the secondary amine group with the double bond of acyl and imino, the obtained dehydroabietyl acylhydrazone compounds (**3a-3p** and **4a-4p**) were stable, did not hydrolyze easily, and had high yields (70–82%).

3.2 Antifungal activity *in vitro* and structure-activity relationship

The inhibitory effect of the dehydroabietyl acylhydrazone compounds (**3a-3p** and **4a-4p**) against *R. solani* was better than that of *F. oxysporum*, *P. capsici, S. sclerotiorum*, and *B. cinerea* (**Table S1**). The inhibitory effect of compounds (**3a-3p** and **4a-4p**) on *R. solani* indicated medium to significant antifungal activities (**Figure 1a** and **Table 1**).

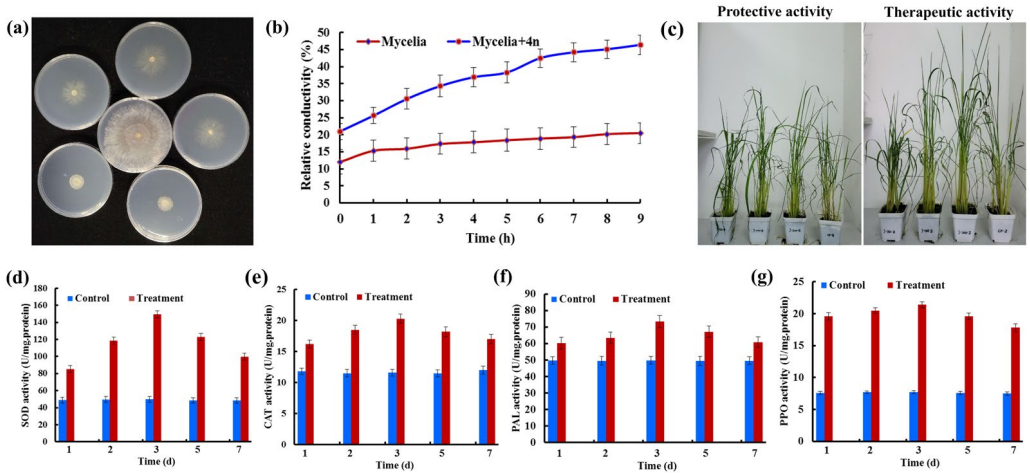

Figure 1. (a) *In vitro* inhibitory activities of **4n** on *R. solani*; (b) Relative conductivity of *R. solani* treated with **4n** and control; (c) Therapeutic activity and protective activity *in vivo* of **4n** on *R. solani* was tested in a greenhouse at 200 mg/L, 100 mg/L and 50 mg/L, respectively. SOD, CAT, PAL, and PPO activity of rice leaf sheaths treated with **4n**; (d) SOD; (e) CAT; (f) PAL; (g) PPO

The antifungal activity of the dehydroabietyl acylhydrazone compounds containing the thiophene structure (**4a-4p**, the EC_{50} value range is 0.981–28.967 mg/L) against *R. solani* was superior to the dehydroabietyl acylhydrazone compounds without the thiophene structure (**3a-3p**, the EC_{50} value range is 87.686–178.156 mg/L). Typically, Compounds **4n-4p** exhibited EC_{50} values ranging from 0.981 to 1.126 mg/L, which were close to the control carbendazim (EC_{50} = 1.045 mg/L), and even at 1.56 mg/L, the *IR* values were still > 50%. Notably, Compound **4n** (EC_{50} = 0.981 mg/L) showed more potent antifungal activity than carbendazim. This phenomenon could be attributed to the *p*-π conjugation effect between the secondary amino group and carbonyl and imino groups of dehydroabietyl acylhydrazone, and the acylhydrazone segment formed a large conjugation system with thiophene rings.[15, 17] In addition, the lone pair of electrons of the sulfur (S) atom in the thiophene heterocyclic compound increased the the electron cloud density on the thiophene ring

and accelerated the electron transfer rate between the thiophene heterocyclic compound and the target site, thus endowed Compounds **4n-4p** with better antifungal effect.[24]

In addition, the antifungal effect of dehydroabietyl acylhydrazone derivatives is related to the different substituents attached to the pharmacophores (acylhydrazone and thiophene ring). In Compounds **3a-3p**, the antifungal activity of compounds, such as X (F, Cl, Br), CF_3, NO_2, with electron-withdrawing groups on the benzene ring is sufficient (**3g-3p**). The EC_{50} value of these compounds was less than Compound **3a** (no group is attached to the benzene ring), and the antifungal effect of compounds containing halogen atom X was optimal. However, the antifungal effect of the compounds (**3b-3f**) with electron-donating groups (OH and R) attached to the benzene ring was weak, and the EC_{50} values were higher than that of Compound **3a**. However, Compounds **3o-3p**, which contain both electron-withdrawing and electron-donating groups, have an antifungal activity that is similar to Compound **3a**. In Compounds **4a-4p**, the antifungal effect of compounds with a benzene ring structure attached to the thiophene ring was higher than the compounds without the benzene ring structure (**4l-4p** > **4a-4k**), and the antifungal effect of compounds with halogen atoms attached to the benzene ring was higher (**4n-4p**). This may be due to the introduction of aromatic ring and electron-withdrawing group to enhance the induction and conjugation effect of the dehydroabietyl acylhydrazone compounds, increasing the electron transfer rate from the donor to the acceptor, and thus improving the antifungal effect.[29-31]

3.3 Effect of dehydroabietyl acylhydrazone (4n) on the cell membrane permeability of *R. solani*

The relative conductivity of *R. solani* was increased remarkbly after treatment

with Compound **4n** compared to control, which meant mycelium electrolyte leakage (**Figure 1b**). In addition, the relative conductivity of *R. solani* increased with the prolonged treatment time of Compound **4n**. These results suggested that Compound **4n** increased the cell membrane permeability, and the cell membrane might be the target site of **4n** on *R. solani*.

3.4 Antifungal activity *in vivo* on *R. solani*

The control effect (*CE*, protective activity and therapeutic activity) of Compound **4n** on *R. solani* was tested in an indoor pot experiment (**Figure 1c** and **Table S2**). The results indicated that **4n** had better therapeutic activity than protective activity. The therapeutic efficacy value of **4n** on *R. solani* was 77.54%, 67.05% and 56.40% at 200 mg/L, 100 mg/L and 50 mg/L, respectively, which was better than the 75.37%, 62.09% and 54.07% of carbendazim. The protective efficacy value of **4n** on *R. solani* was 69.24%, 50.60% and 46.93%, respectively, which was lower than 71.85%, 55.24% and 48.26% of carbendazim.

3.5 Effects of dehydroabietyl acylhydrazone (4n) on defense enzyme induction activity in rice leaf sheaths

SOD, CAT, PAL, and PPO are the main components of the protective cell enzyme system against the damage caused by active oxygen.[32] These compounds play a critical role in eliminating active oxygen, preventing or reducing the formation of hydroxyl radicals, and delaying plant aging.[33, 34] The SOD and CAT activities in rice leaf sheaths decreased slightly, then increased rapidly, and finally declined at different rates, as shown in **Figure 1d** and **Figure 1e**. The increase in enzyme activity indicated that the initial resistance of the rice plant was stimulated, which helped in eliminating or maintaining the balance of the active oxygen, protecting the normal cells, and improving resistance. The enzyme activity of the treatment with **4n** was lower than

the control that could be from the rapid accumulation of active oxygen; the enzyme could not eliminate the burst of active oxygen thereby causing severe damage to the cell membrane system of the rice plant.

PAL and PPO are closely related to the metabolism of phenols in plants. They can provide a phenylpropane carbon skeleton or carbon bridge for the synthesis of plant defensins and lignin to kill or inhibit the propagation of pathogens or improve the mechanical strength of the cell wall.[35] Subsequently, the PAL and PPO activities of the rice leaf sheaths increased rapidly and then decreased significantly after pathogen infection, indicating that the initial resistance period of rice plants was short (**Figure 1f** and **Figure 1g**). However, after treatment with **4n**, the PAL and PPO activity increased to varying degrees over a long span of time, followed by a slow decline, thereby demonstrating **4n** as beneficial to the continuous disease resistance of rice plants.

3.6 The influence of dehydroabietyl acylhydrazone (4n) on the mycelial morphology of *R. solani*

In the control group, the mycelium grew vigorously, stretched well, and was smooth and full (**Figure 2a** and **Figure 2b**). However, the surface of the mycelium was rough, shriveled, and deformed after treatment with **4n** (**Figure 2c** and **Figure 2d**). Moreover, the growth of mycelium was disordered. The above results showed that dehydroabietyl acylhydrazone (**4n**) had an inhibitory effect on the mycelial morphology of *R. solani*.

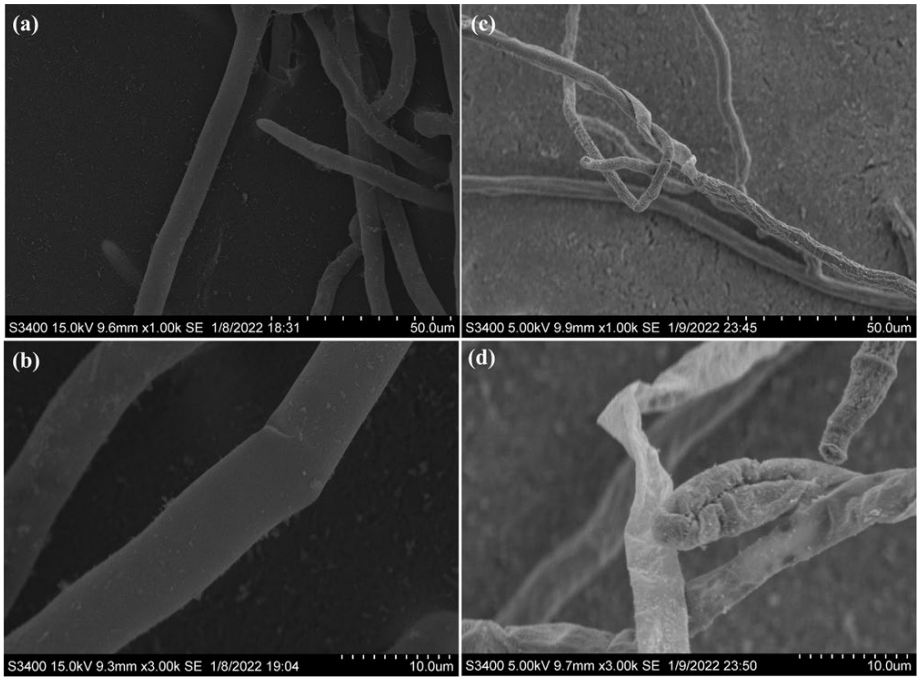

Figure 2. Effect of **4n** on mycelial morphology in *R. solani*: (a, b) Control (1.00 K and 3.00 K times, respectively); (c, d) Treated with **4n** (1.00 K and 3.00 K times, respectively)

3.7 The influence of dehydroabietyl acylhydrazone (4n) on the mycelial microstructure of *R. solani*

The mycelial microstructure of *R. solani* was observed by TEM (**Figure 3a**, **Figure 3b** and **Figure 3c**, **Figure 3d** are horizontal-vertical sections of *R. solani* fungal cells, respectively). In the control group, the cell wall of the hyphae was intact, the cytoplasm was distributed evenly, and the organelles were evenly distributed and clearly visible (**Figure 3a** and **Figure 3c**). After treatment with the EC_{50} concentration of **4n**, the hyphal cells began to pyknosis, large vacuoles appeared, and the organelles were partially blurred (**Figure 3b** and **Figure 3d**).

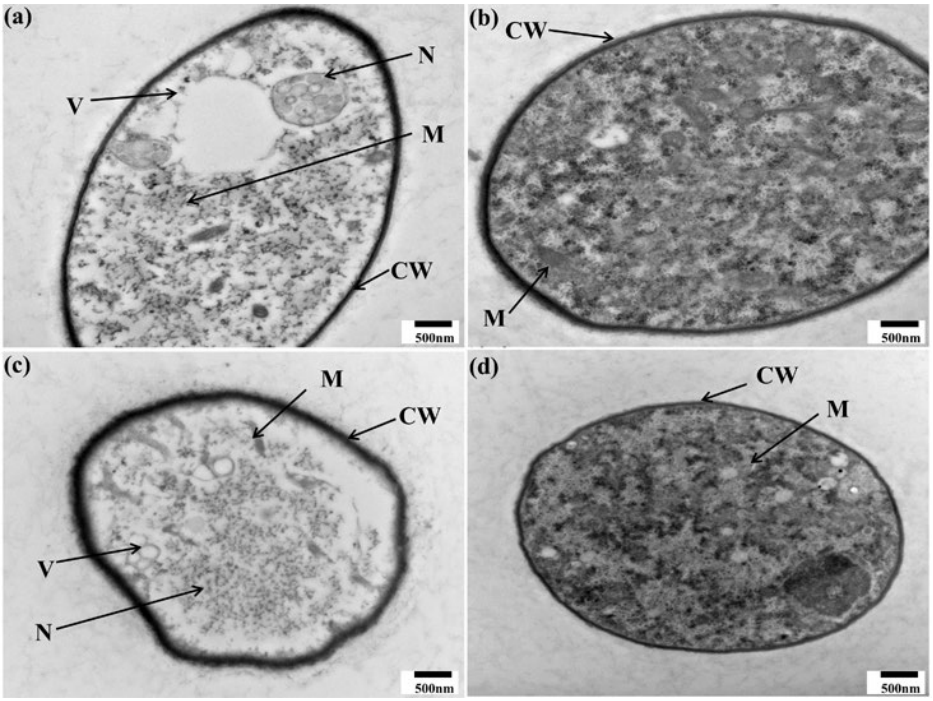

Figure 3. Mycelial microstructure of *R. solani*: (a, c) Control; (b, d) Treated with **4n**. CW, cell wall; M, mitochondria; N, nucleus; V, vesicle

3.8 The analysis of confocal laser scanning microscope of *R. solani*

Reactive oxygen species (ROS) are metabolic byproducts of oxygen, and mitochondria are the main target of ROS. The generation and accumulation of ROS can induce the opening of the permeable pores in the mitochondrial bilayer membrane that leads to apoptosis. The ROS determination results showed that distinct fluorescence was observed in the hyphae of *R. solani* treated with Compound **4n** compared to the untreated hyphae (**Figure 4a** and **Figure 4d**). Compound **4n** can induce production of ROS in fungal cells, which affects the structure or normal physiological function of fungal cells.[36]

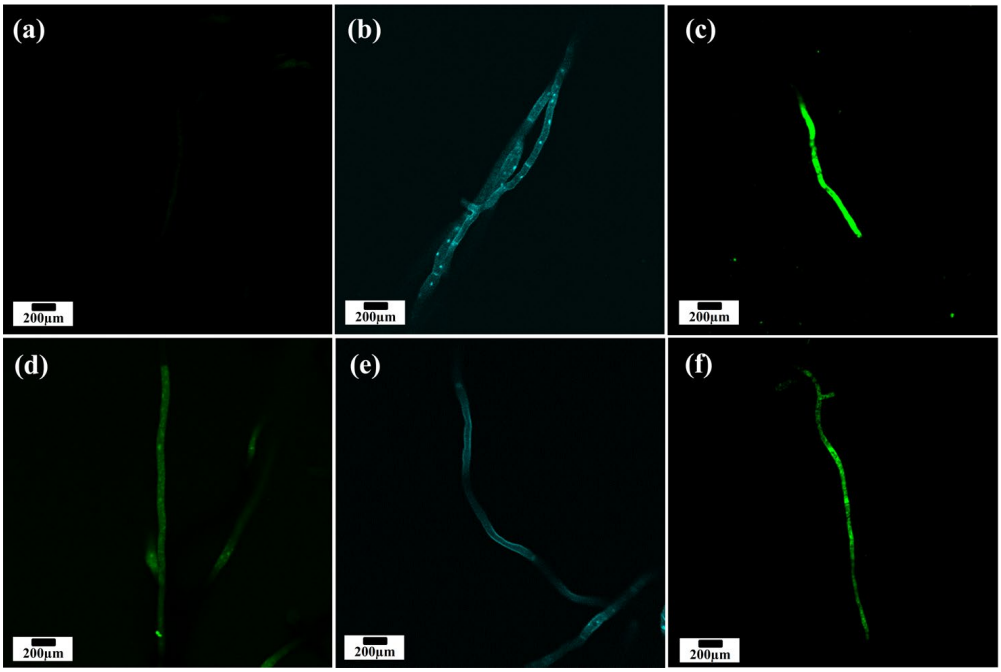

Figure 4. ROS, nuclear morphology and MMP of *R. solani*: (a, b and c) Control; (d, e and f) Treated with **4n**

The results of nuclear fluorescence staining showed that different drug treatments had certain effects on fungal nuclei. As shown in **Figure 4b**, untreated hyphal nuclei showed uniform blue fluorescence, and distinct discrete signals could be observed. The nuclei of hyphal cells treated with Compound **4n** decreased, and the discrete signal of nuclei was weak and showed dense dyeing or fragmented dyeing **(Figure 4e**).[37]

Mitochondria are the main sites for fungal cells to generate adenosine triphosphate (ATP) and are important organelles that promote cell energy conversion and participate in cell apoptosis. Therefore, the stability of MMP is conducive to maintaining the normal physiological functions of cells. As shown in **Figure 4c** and **Figure 4f**, the fluorescence intensity of *R. solani* treated with **4n** decreased, indicating that Compound **4n** could act on the mitochondria of fungal cells, which was also consistent with the previous ROS fluorescence analysis.[38]

3.9 Analysis of QSAR

The correlation and the molecular descriptors of the antifungal activity of rosin-base acylhydrazone compounds against *R. solani* were analyzed by the established QSAR model. The best model with four structural descriptors was then screened out according to the breakpoint rules (**Figure 5a**, **Table 2** and **Table S3**).[39, 40] The "leave-one-out" cross-validation indicate that the best model has better stability and the results are listed in **Table S4**. Finally, the antifungal activity of the dehydroabietyl acylhydrazone derivatives was predicted by the best model. The difference (less than 5%) between the predicted and the experimental results was small, indicating that the model has good predictive ability (**Figure 5b** and **Table S5**).

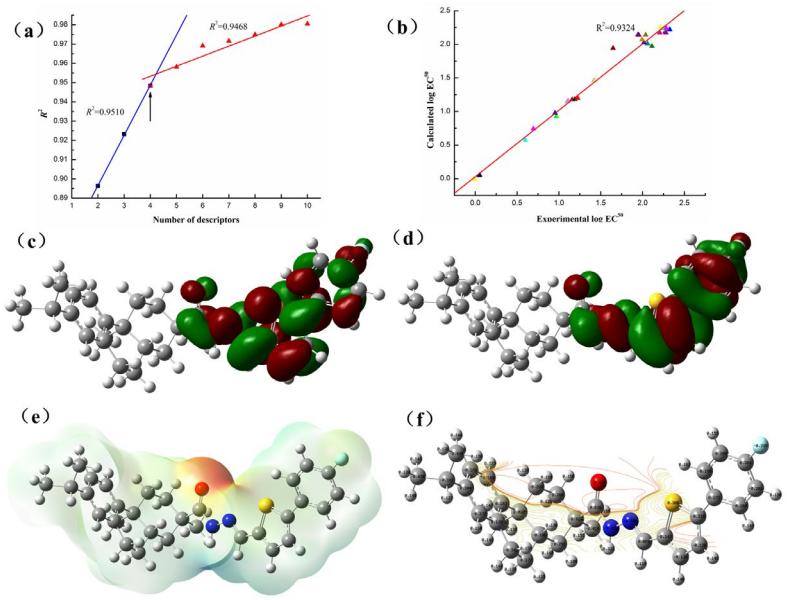

Figure 5. The QSAR analysis: (a) Breakpoint rule; (b) The comparison between predicted and experimental results; (c, d) *HOMO* and *LUMO* maps, respectively; (e) MEP map; (f) Charge distribution and contour plot

Four descriptors in the optimal QSAR model that are closely related to antifungal effect on *R. solani* were identified (**Table 2**). The most important descriptor is the energy gap (*HOMO-LUMO*) between the highest occupied molecular orbital (*HOMO*) and the lowest unoccupied orbital (*LUMO*) in the atomic unit. *HOMO-LUMO* is a quantitative chemical descriptor.[41] The frontier orbital energies of Compound **4n**

influenced significantly on the antifungal activity of *R. solani* according to molecular orbital theory (**Figure 5c** and **Figure 5d**). In addition, the electron cloud is mainly concentrated on the acyl ketone group. Therefore, when the donor and acceptor establish contact, this part of the structure of Compound **4n** can stably donate electrons.[42-44] The dipole moment (*DM*) can reflect the reactivity of the Compound **4n** with the receptor, including the reaction rate and direction.[45, 46]

The min net atomic charge for an N atom (q^{N}_{min}) and the max net atomic charge (q_{max}) are electrostatic descriptors.[47, 48] The molecular electrostatic potential (MEP) map reflects the size of the electron charge density of the compound (**Figure 5e**). The red color indicates a high energy level and large number of electrons. When the drug molecules exert their efficacy, they mainly provide electrons to acceptor.[49-51] Furthermore, the charge distribution and contour plot of **4n** showed that the charge density of carbonyl oxygen in the acylhydrazone group was high (**Figure 5f**), indicating that the electron is given mainly by this part in the binding reaction with the receptor. Conversely, the blue color on the thiophene ring is shown on the MEP plot that indicates the abundant positive charge on the thiophene ring.[52, 53]

4 CONCLUSION

Two series of dehydroabietyl acylhydrazone compounds (**3a-3p** and **4a-4p**) were synthesized and their antifungal effect on *R. solani*, *F. oxysporum*, *P. capsici, S. sclerotiorum*, and *B. cinerea* were evaluated. The dehydroabietyl acylhydrazone derivatives containing a thiophene ring (**4a-4p**) showed a better inhibition effect on *R. solani* than those without the thiophene structure (**3a-3p**). Among these compounds, **4n** exhibits the optimal activity. The primary action mechanism of **4n** on rice *R. solani* demonstrated that it could affect the mycelial morphology and microstructure, cause the generation of ROS in fungal cells and mitochondrial dysfunction, and damage the

fungal nuclei. The antifungal activity *in vivo* results indicated that **4n** presented a better therapeutic effect on rice plants. Moreover, **4n** can also improve the activities of defense enzymes (SOD, CAT, PAL, and PPO) in rice leaf sheaths to enhance the resistance of rice plants. The QSAR analysis suggested that the descriptors of **4n** (*HOMO-LUMO*, *DM*, q^{N}_{min}, and q_{max}) were notably related to the antifungal activity against *R. solani*.

ACKNOWLEDGEMENTS

This work was supported by the National Natural Science Foundation of China [grant numbers 31870555]; Innovation and Entrepreneurship Training Program for College Students [grant numbers 202110712077]

SUPPORTING INFORMATION

Experimental methods and instruments, structural characterization, antifungal activity and QSAR data of the compounds.

Conflict of Interest Declaration

The authors declare that there are no conflicts of interest.

REFERENCES

1 DeLiberto ST and Werner SJ, Review of anthraquinone applications for pest management and agricultural crop protection. *Pest Manag Sci* **72**:1813-1825 (2016).

2 Ristaino JB, Anderson PK, Bebber DP, Brauman KA, Cunniffe NJ, Fedoroff NV, et al., The persistent threat of emerging plant disease pandemics to global food security. *P Natl Acad Sci* **118**:e2022239118 (2021).

3 Li K, Xing R, Liu S, Qin Y, Meng X and Li P, Microwave-assisted degradation of chitosan for a possible use in inhibiting crop pathogenic fungi. *Int J Biol Macromol* **51**:767-773 (2012).

4 Anderson AJ, McLean JE, Jacobson AR and Britt DW, CuO and ZnO Nanoparticles modify interkingdom cell signaling processes relevant to crop production. *J Agr Food Chem* **66**:6513-6524 (2018).

5 Ajayi-Oyetunde OO and Bradley CA, Rhizoctonia solani: taxonomy, population biology and management of rhizoctonia seedling disease of soybean. *Plant Pathol* **67**:3-17 (2018).

6 Ma YN, Xu FR, Chen CJ, Li QQ, Wang MZ, Cheng YX, et al., The beneficial use of essential oils from buds and fruit of Syzygium aromaticum to combat pathogenic fungi of Panax notoginseng. *Ind Crop Prod* **133**:185-192 (2019).

7 Verger PJP and Boobis AR, Reevaluate pesticides for food security and safety. *Science* **341**:717 (2013).

8 Phillips MWA, Agrochemical industry development, trends in R&D and the impact of regulation. *Pest Manag Sci* **76**:3348-3356 (2020).

9 Clements J, Schoville S, Clements A, Amezian D, Davis T, Sanchez-Sedillo B, et al., Agricultural fungicides inadvertently influence the fitness of Colorado potato beetles, Leptinotarsa decemlineata, and their susceptibility to insecticides. *Sci Rep* **8**:13282 (2018).

10 Li D, Luong TTM, Dan WJ, Ren Y, Nien HX, Zhang AL, et al., Natural products as sources of new fungicides (IV): Synthesis and biological evaluation of isobutyrophenone analogs as potential inhibitors of class-II fructose-1,6-bisphosphate aldolase. *Bioorg Med Chem Lett* **26**:386-393 (2018).

11 Koehler AM and Shew HD, Effects of fungicide applications on root-infecting microorganisms and overwintering survival of perennial stevia. *Crop Prot* **120**:13-20 (2019).

12 Guo Z, Ma W, Gu H, Feng Y, He Z, Chen Q, et al., pH-Switchable and

self-healable hydrogels based on ketone type acylhydrazone dynamic covalent bonds. *Soft Matter* **13**:7371-7380 (2017).

13 Bi H, Wang S, Zhou W, Zhuang Y and Liu T, Producing gram-scale unnatural rosavin analogues from glucose by engineered Escherichia coli. *ACS Synth Biol* **8**:1931-1940 (2019).

14 Mao S, Wu C, Gao Y, Hao J, He X, Tao P, et al., Pine rosin as a valuable natural resource in the synthesis of fungicide candidates for controlling Fusarium oxysporum on cucumber. *J Agr Food Chem* **69**:6475-6484 (2021).

15 Guilherme FD, Simonetti JÉ, Folquitto LRS, Reis ACC, Oliver JC, Dias ALT, et al., Synthesis, chemical characterization and antimicrobial activity of new acylhydrazones derived from carbohydrates. *J Mol Struct* **1184**:349-356 (2019).

16 Xiao G, Wang Y, Zhang H, Chen L and Fu S, Facile strategy to construct a self-healing and biocompatible cellulose nanocomposite hydrogel via reversible acylhydrazone. *Carbohyd Polym* **218**:68-77 (2019).

17 Santhiya K, Sen SK, Natarajan R, Shankar R and Murugesapandian B, D–A–D Structured bis-acylhydrazone exhibiting aggregation-induced emission, mechanochromic luminescence, and Al (III) detection. *J Org Chem* **83**:10770-10775 (2018).

18 Zhang J, Wei C, Li S, Hu D, Song B, Discovery of novel bis-sulfoxide derivatives bearing acylhydrazone and benzothiazole moieties as potential antibacterial agents. *Pestic Biochem Physiol* **167**:104605 (2020).

19 Lee SW, Choi JH, Cho SK, Yu HA, Abd El-Aty AM and Shim JH, Development of a new QuEChERS method based on dry ice for the determination of 168 pesticides in paprika using tandem mass spectrometry. *J Chromatogr A* **1218**:4366-4377 (2011).

20 Ishibashi M, Izumi Y, Sakai M, Ando T, Fukusaki E and Bamba T, High-throughput simultaneous analysis of pesticides by supercritical fluid chromatography coupled with high-resolution mass spectrometry. *J Agr Food Chem* **63**:4457-4463 (2015).

21 Hamadache M, Benkortbi O, Hanini S, Amrane A, Khaouane L and Si Moussa C, A quantitative structure activity relationship for acute oral toxicity of pesticides on rats: Validation, domain of application and prediction. *J Hazard Mater* **303**:28-40 (2016).

22 Masahiko T, Fumiyuki K, Keisuke S, Shuichi O and Michio S, Germination and appressorium formation of Pyricularia oryzae Cavara can be inhibited by reduced concentration of Blasin®Flowable with carbon dioxide microbubbles. *J Integr Agr* **17**:2024-2030 (2018).

23 El-Mekabaty A, Habib OMO, Moawad EB and Abo-Ouf RM, Efficient syntheses of some new thiophene-based heterocycles. *J Heterocyclic Chem* **54**:561-569 (2017).

24 Fokialakis N, Cantrell CL, Duke SO, Skaltsounis AL and Wedge DE, Antifungal activity of thiophenes from Echinops ritro. *J Agr Food Chem* **54**:1651-1655 (2006).

25 Yang Z, Sun Y, Liu Q, Li A, Wang W, Gu W, Design, synthesis, and antifungal activity of novel thiophene/furan-1, 3, 4-oxadiazole carboxamides as potent succinate dehydrogenase inhibitors. *J Agr Food Chem* **69**:13373-13385 (2021).

26 Ortíz-López FJ, Monteiro MC, González-Menéndez V, Tormo JR, Genilloud O, Bills GF, et al., Cyclic colisporifungin and linear cavinafungins, antifungal lipopeptides isolated from Colispora cavincola. *J Nat Prod* **78**:468-475 (2015).

27 Cong Y, Fan H, Ma Q, Lu Y, Xu L, Zhang P, et al., Mixed culture fermentation

between Rhizopus nigricans and Trichoderma pseudokoningii to control cucumber Fusarium wilt. *Crop Prot* **124**:104857 (2019).

28 Gao Y, Xu R, Gu S, Chen K, Li J, He X, et al., Discovery of natural rosin derivatives containing oxime ester moieties as potential antifungal agents to control tomato gray mold caused by *Botrytis cinerea*. *J Agr Food Chem* **70**: 5551–5560 (2022).

29 Owen WJ, Sullenberger MT, Loso MR, Meyer KG and Slanec TJ, Synthesis and antifungal activity of 3-aryl-1,2,4-triazin-6-one derivatives. *Pest Manag Sci* **71**:83-90 (2015).

30 Nishiwaki H, Nakazaki S, Akiyama K and Yamauchi S, Structure-antifungal activity relationship of fluorinated dihydroguaiaretic acid derivatives and preventive activity against Alternaria alternata Japanese pear pathotype. *J Agr Food Chem* **65**:6701-6707 (2017).

31 Wang SQ, Wang YF and Xu Z, Tetrazole hybrids and their antifungal activities. *Eur J Med Chem* **170**:225-234 (2019).

32 Aljuhani N, Whittal RM, Khan SR and Siraki AG, Phenylbutazone oxidation via Cu, Zn-SOD peroxidase activity: An EPR study. *Chem Res Toxicol* **28**:1476-1483 (2015).

33 Yingsanga P, Srilaong V, Kanlayanarat S, Noichinda S and McGlasson WB, Relationship between browning and related enzymes (PAL, PPO and POD) in rambutan fruit (Nephelium lappaceum Linn.) cvs. Rongrien and See-Chompoo. *Postharvest Biol Tec* **50**:164-168 (2008).

34 Jiang S, Han S, He D, Cao G, Fang K, Xiao X, et al., The accumulation of phenolic compounds and increased activities of related enzymes contribute to early defense against walnut blight. *Physiol Mol Plant P* **108**:101433 (2019).

35 Ma C, Liu H, Guo H, Musante C, Coskun SH, Nelson BC, et al., Defense mechanisms and nutrient displacement in Arabidopsis thaliana upon exposure to CeO_2 and In_2O_3 nanoparticles. *Environ Sci-Nano* **3**:1369-1379 (2016).

36 Nosaka Y, Nosaka AY, Generation and detection of reactive oxygen species in photocatalysis. *Chem Rev* **117**:11302-11336 (2017).

37 Kim JK, Louhghalam A, Lee G, Schafer BW, Wirtz D, and Kim DH, Nuclear lamin A/C harnesses the perinuclear apical actin cables to protect nuclear morphology. *Nat Commun* **8**:1-13 (2017).

38 Rouco L, Alvariño R, Alfonso A, Romero MJ, Pedrido R, and Maneiro M, Neuroprotective effects of fluorophore-labelled manganese complexes: Determination of ROS production, mitochondrial membrane potential and confocal fluorescence microscopy studies in neuroblastoma cells. *J Inorg Biochem* **227**:111670 (2022).

39 Wang Z, Song J, Han Z, Jiang Z, Zheng W, Chen J, et al., Quantitative structure−activity relationship of terpenoid aphid antifeedants. *J Agr Food Chem* **56**:11361-11366 (2008).

40 Huang YM, Banerjee S, Crone DE, Schenkelberg CD, Pitman DJ, Buck PM, et al., Toward computationally designed self-reporting biosensors using leave-one-out green fluorescent protein. *Biochemistry* **54**:6263-6273 (2015).

41 Kawai K, Hayashi M and Majima T, HOMO energy gap dependence of hole-transfer kinetics in DNA. *J Am Chem Soc* **134**:4806-4811 (2012).

42 AlAbbad S, Sardot T, Lekashvili O, Decato D, Lelj F, Ross JBA, et al., Trans influence and substituent effects on the HOMO-LUMO energy gap and Stokes shift in Ru mono-diimine derivatives. *J Mol Struct* **1195**:620-631 (2019).

43 Barim E and Akman F, Synthesis, characterization and spectroscopic investigation

of N-(2-acetylbenzofuran-3-yl)acrylamide monomer: Molecular structure, HOMO–LUMO study, TD-DFT and MEP analysis. *J Mol Struct* **1195**:506-513 (2019).

44 Santos ES, Reis VS, Guimarães L and Nascimento CS, Molecular wires formed from native and push-pull derivatives polypyrroles and β-cyclodextrins: A HOMO-LUMO gap theoretical investigation. *Chem Phys Lett* **730**:141-146 (2019).

45 Liang W, Li X, Dalton LR, Robinson BH and Eichinger BE, Solvents level dipole moments. *J Phys Chem B* **115**:12566-12570 (2011).

46 McNamara KD and Zoellner RW, The effects of substituent position and orientation on the structures and dipole moments of the cyanocyclohexanes using density functional theory calculations. *Comput Theor Chem* **1170**:112622 (2019).

47 Nusser T, Balogh T and Náray-Szabó G, The average molecular electrostatic field as a QSAR descriptor: 5. Hydrophobicity indices for small molecules. *J Mol Struct* **297**:127-132 (1993).

48 González-Díaz H, Molina R and Uriarte E, Markov entropy backbone electrostatic descriptors for predicting proteins biological activity. *Bioorg Med Chem Lett* **14**:4691-4695 (2004).

49 Sandhiya L and Senthilkumar K, A theoretical probe on the non-covalent interactions of sulfadoxine drug with pi-acceptors. *J Mol Struct* **1074**:157-167 (2014).

50 Behzadi H, Roonasi P, van der Spoel D and Manzetti S, Relationship between electronic properties and drug activity of seven quinoxaline compounds: A DFT study. *J Mol Struct* **1091**: 196-202 (2015).

51 Matta CF and Arabi AA. Electron-density descriptors as predictors in quantitative

structure--activity/property relationships and drug design. *Future Med Chem* **3**:969-94 (2011).

52 Jalan A, Ashcraft RW, West RH and Green WH, Predicting solvation energies for kinetic modeling. *Annu Rep Prog Chem, Sect C: Phys Chem* **106**:211-258 (2010).

53 Zarzycki P, Chatman S, Preočanin T and Rosso KM, Electrostatic potential of specific mineral faces. *Langmuir* **27**:7986-7990 (2011).

Table 1 Antifungal activity of dehydroabietyl acylhydrazone derivatives (**3a-3p** and **4a-4p)** against *Rhizoctonia solani*

compound	*IR* (%) at a concentration of (mg/L) ± standard deviation (SD; n ⩾ 3)										EC_{50}	*y*=a+b*x*	R^2	log EC_{50}
	500.00	200.00	100.00	50.00	25.00	12.50	6.25	3.13	1.56	0.78				
3a	100.00 ± 0.00 a	67.00 ± 1.12 c	32.00 ± 0.72 c	14.50 ± 0.15 d	8.50 ± 0.05 f	3.80 ± 0.03 d	/	/	/	/	154.225	*y*=-3.054+0.209*x*	0.953	2.188
3b	100.00 ± 0.00 a	62.00 ± 0.99 c	28.00 ± 0.37 d	13.10 ± 0.17 d	7.20 ± 0.08 f	/	/	/	/	/	165.644	*y*=-3.334+0.230*x*	0.986	2.219
3c	100.00 ± 0.00 a	61.50 ± 1.08 c	27.80 ± 0.25 d	13.00 ± 0.16 d	7.10 ± 0.07 f	/	/	/	/	/	166.587	*y*=-3.340+0.231*x*	0.986	2.222
3d	99.00 ± 1.96 a	59.50 ± 1.10 c	30.00 ± 0.37 c	13.80 ± 0.09 d	7.20 ± 0.08 f	/	/	/	/	/	171.826	*y*=-2.907+0.221*x*	0.994	2.235
3e	99.00 ± 2.33 a	58.50 ± 0.98 d	29.90 ± 0.34 c	13.50 ± 0.12 d	7.10 ± 0.04 f	/	/	/	/	/	173.674	*y*=-2.915+0.222*x*	0.994	2.240
3f	99.00 ± 2.52 a	56.50 ± 0.92 d	28.80 ± 0.27 d	12.80 ± 0.20 d	6.90 ± 0.05 f	/	/	/	/	/	178.156	*y*=-2.953+0.224*x*	0.994	2.251
3g	100.00 ± 0.00 a	73.10 ± 1.28 c	38.00 ± 0.56 b	19.25 ± 0.18 d	11.80 ± 0.15 e	5.30 ± 0.06 d	/	/	/	/	138.178	*y*=-2.763+0.190*x*	0.954	2.140
3h	100.00 ± 0.00 a	73.20 ± 1.55 c	38.10 ± 0.61 b	19.45 ± 0.20 d	11.88 ± 0.09 e	5.40 ± 0.05 d	/	/	/	/	137.843	*y*=-2.752+0.189*x*	0.955	2.139
3i	100.00 ± 0.00 a	73.00 ± 1.26 c	37.90 ± 0.42 b	19.15 ± 0.21 d	11.70 ± 0.08 e	5.25 ± 0.04 d	/	/	/	/	138.467	*y*=-2.769+0.190*x*	0.954	2.141
3j	100.00 ± 0.00 a	98.50 ± 2.13 a	49.60 ± 0.95 b	33.00 ± 0.50 c	17.90 ± 0.17 e	9.50 ± 0.06 d	5.30 ± 0.04 d	/	/	/	87.686	*y*=-2.508+0.184*x*	0.974	1.943
3k	100.00 ± 0.00 a	95.30 ± 1.84 a	49.20 ± 0.91 b	30.10 ± 0.41 c	16.00 ± 0.13 e	8.50 ± 0.06 d	5.00 ± 0.06 d	/	/	/	93.877	*y*=-2.539+0.183*x*	0.978	1.973
3l	100.00 ± 0.00 a	93.50 ± 1.79 b	41.00 ± 0.73 b	30.00 ± 0.43 c	15.00 ± 0.14 e	9.00 ± 0.07 d	5.00 ± 0.05 d	/	/	/	102.081	*y*=-2.525+0.180*x*	0.968	2.009
3m	100.00 ± 0.00 a	90.10 ± 1.66 b	41.90 ± 0.69 b	28.00 ± 0.27 c	15.20 ± 0.15 e	9.50 ± 0.08 d	5.00 ± 0.04 d	/	/	/	106.450	*y*=-2.461+0.175*x*	0.967	2.027
3n	100.00 ± 0.00 a	84.00 ± 1.84 b	40.50 ± 0.55 b	25.10 ± 0.43 c	14.00 ± 0.10 e	8.90 ± 0.05 d	/	/	/	/	117.903	*y*=-2.606+0.182*x*	0.988	2.072
3o	100.00 ± 0.00 a	69.10 ± 1.13 c	34.05 ± 0.44 c	15.00 ± 0.17 d	9.55 ± 0.08 f	3.95 ± 0.02 d	/	/	/	/	149.238	*y*=-2.991+0.205*x*	0.950	2.174
3p	100.00 ± 0.00 a	69.00 ± 1.08 c	33.90 ± 0.41 c	14.99 ± 0.13 d	9.50 ± 0.07 f	3.90 ± 0.03 d	/	/	/	/	149.514	*y*=-2.996+0.205*x*	0.950	2.175
4a	100.00 ± 0.00 a	100.00 ± 0.00 a	98.30 ± 2.01 a	79.80 ± 1.48 b	56.90 ± 0.85 d	41.90 ± 0.87 c	33.00 ± 0.45 c	19.00 ± 0.13 b	/	/	25.386	*y*=-1.837+0.129*x*	0.986	1.405
4b	100.00 ± 0.00 a	100.00 ± 0.00 a	95.00 ± 1.95 a	77.10 ± 1.42 b	54.33 ± 0.92 d	39.50 ± 1.05 c	31.00 ± 0.41c	17.50 ± 0.19 b	/	/	28.949	*y*=-1.799+0.126*x*	0.963	1.462
4c	100.00 ± 0.00 a	100.00 ± 0.00 a	95.00 ± 1.89 a	77.30 ± 1.40 b	54.00 ± 0.83 d	39.00 ± 0.72 c	31.20 ± 0.58 c	17.80 ± 0.26 b	/	/	28.967	*y*=-1.800+0.126*x*	0.965	1.462
4d	100.00 ± 0.00 a	100.00 ± 0.00 a	95.30 ± 2.11 a	77.20 ± 1.40 b	54.00 ± 0.82 d	39.10 ± 0.81 c	31.00 ± 0.60 c	17.50 ± 0.12 b	/	/	28.859	*y*=-1.814+0.126*x*	0.967	1.460
4e	100.00 ± 0.00 a	100.00 ± 0.00 a	100.00 ± 0.00 a	98.00 ± 1.97 a	69.00 ± 1.28 c	51.50 ± 0.89 c	42.00 ± 0.65 b	32.25 ± 0.62 a	24.00 ± 0.27 b	/	14.011	*y*=-1.450+0.126*x*	0.979	1.146
4f	100.00 ± 0.00 a	100.00 ± 0.00 a	100.00 ± 0.00 a	97.49 ± 2.02 a	68.10 ± 1.10 c	51.00 ± 0.91c	41.20 ± 0.83 b	32.00 ± 0.71 a	23.80 ± 0.30 b	/	14.385	*y*=-1.453+0.126*x*	0.982	1.158
4g	100.00 ± 0.00 a	100.00 ± 0.00 a	100.00 ± 0.00 a	96.49 ± 1.96 a	67.20 ± 1.05 c	50.00 ± 1.02 c	40.14 ± 0.72 b	31.00 ± 0.48 a	22.50 ± 0.29 b	/	15.050	*y*=-1.479+0.126*x*	0.984	1.178
4h	100.00 ± 0.00 a	100.00 ± 0.00 a	100.00 ± 0.00 a	96.09 ± 1.89 a	67.00 ± 0.92 c	50.10 ± 0.84 c	40.14 ± 0.67 b	30.80 ± 0.72 a	22.00 ± 0.36 b	/	15.204	*y*=-1.479+0.126*x*	0.984	1.181
4i	100.00 ± 0.00 a	100.00 ± 0.00 a	100.00 ± 0.00 a	95.09 ± 1.91 a	66.00 ± 1.21 c	49.50 ± 0.88 c	39.64 ± 0.54 b	29.00 ± 0.52 a	21.50 ± 0.35 b	/	15.823	*y*=-1.498+0.125*x*	0.984	1.199
4j	100.00 ± 0.00 a	100.00 ± 0.00 a	100.00 ± 0.00 a	100.00 ± 0.00 a	89.00 ± 1.53 b	73.00 ± 1.36 b	50.60 ± 0.92 b	37.10 ± 0.59 a	24.50 ± 0.42 b	/	8.414	*y*=-1.498+0.141*x*	0.952	0.925
4k	100.00 ± 0.00 a	100.00 ± 0.00 a	100.00 ± 0.00 a	100.00 ± 0.00 a	86.00 ± 1.81 b	70.44 ± 1.13 b	46.30 ± 0.75 b	32.00 ± 0.40 a	23.50 ± 0.38 b	/	9.470	*y*=-1.573+0.141*x*	0.947	0.976
4l	100.00 ± 0.00 a	100.00 ± 0.00 a	100.00 ± 0.00 a	100.00 ± 0.00 a	100.00 ± 0.00 a	87.60 ± 1.53 a	72.12 ± 1.26 a	46.08 ± 0.66 a	37.30 ± 0.52 a	27.18 ± 0.33 b	3.730	*y*=-0.994+0.147*x*	0.962	0.572
4m	100.00 ± 0.00 a	100.00 ± 0.00 a	100.00 ± 0.00 a	100.00 ± 0.00 a	99.00 ± 2.11 a	85.00 ± 1.66 a	67.00 ± 1.20 a	40.00 ± 0.54 a	26.00 ± 0.37 b	/	5.529	*y*=-1.790+0.169*x*	0.988	0.743
4n	100.00 ± 0.00 a	100.00 ± 0.00 a	100.00 ± 0.00 a	100.00 ± 0.00 a	100.00 ± 0.00 a	98.21 ±1.98 a	90.92 ± 1.83 a	71.32 ± 1.23 a	56.94 ± 0.92 a	45.62 ± 1.00 a	0.981	*y*=-0.400+0.173*x*	0.984	-0.008
4o	100.00 ± 0.00 a	100.00 ± 0.00 a	100.00 ± 0.00 a	100.00 ± 0.00 a	100.00 ± 0.00 a	96.82 ± 2.11 a	89.64 ± 1.73 a	69.32 ± 1.06 a	54.74 ± 1.30 a	43.81 ± 0.91 a	1.103	*y*=-0.405+0.166*x*	0.963	0.043
4p	100.00 ± 0.00 a	100.00 ± 0.00 a	100.00 ± 0.00 a	100.00 ± 0.00 a	100.00 ± 0.00 a	96.52 ± 1.89 a	89.35 ± 1.79 a	69.12 ± 1.06 a	54.24 ± 1.15 a	43.52 ± 0.83 a	1.126	*y*=-0.405+0.165*x*	0.959	0.052
carbendazim	100.00 ± 0.00 a	100.00 ± 0.00 a	100.00 ± 0.00 a	100.00 ± 0.00 a	100.00 ± 0.00 a	97.37 ± 1.91 a	90.12 ± 1.78 a	70.02 ± 1.02 a	56.14± 0.98 a	44.22 ± 0.79 a	1.045	*y*=-0.398+0.168*x*	0.971	

Values in columns followed by similar letters were not significantly different according to Fisher's protected LSD test ($P < 0.05$)

Table 2 QSAR model with four descriptors

descriptor No.	*X*	± *ΔX*	*t*-test	descriptor
0	1.3715e+01	2.7521e+00	4.9836	intercept
1	-5.9544e-02	7.1897e-03	-8.2818	*HOMO-LUMO* †
2	-6.3093e-01	4.1510e-02	-15.1993	q^{N}_{min} ‡
3	-4.3352e+00	1.2512e+00	-3.4649	*H* §
4	1.3946e+01	7.2922e+00	1.9124	*DM* ¶

† Energy gap between *HOMO* and *LUMO*. ‡ Mix net atomic charge for a N atom. § Max net atomic charge . ¶ Dipole moment.

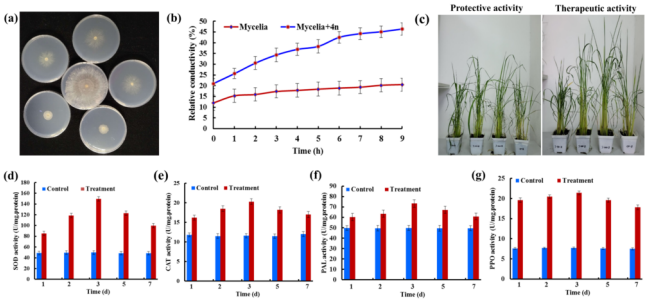

PS_7232_Figure 1.tif

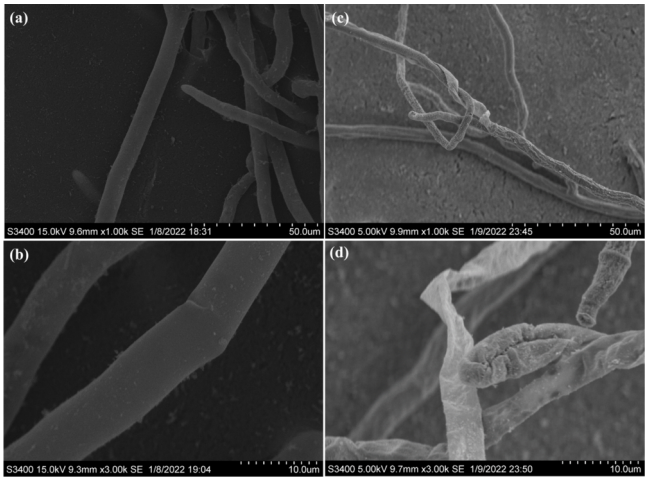

PS_7232_Figure 2.tif

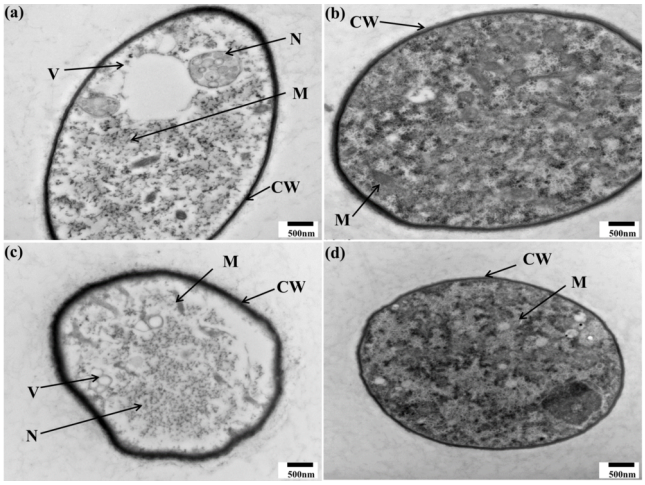

PS_7232_Figure 3.tif

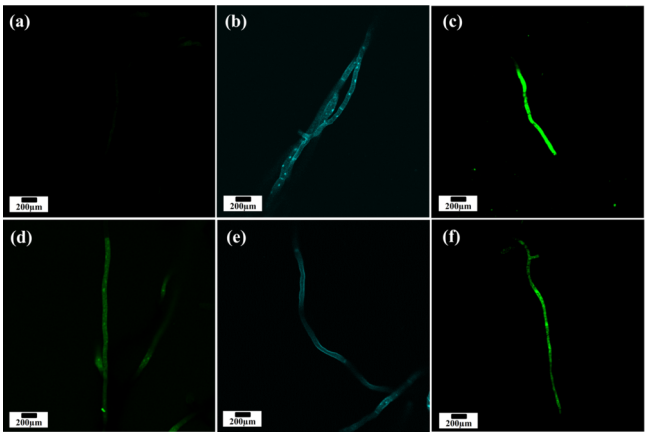

PS_7232_Figure 4.tif

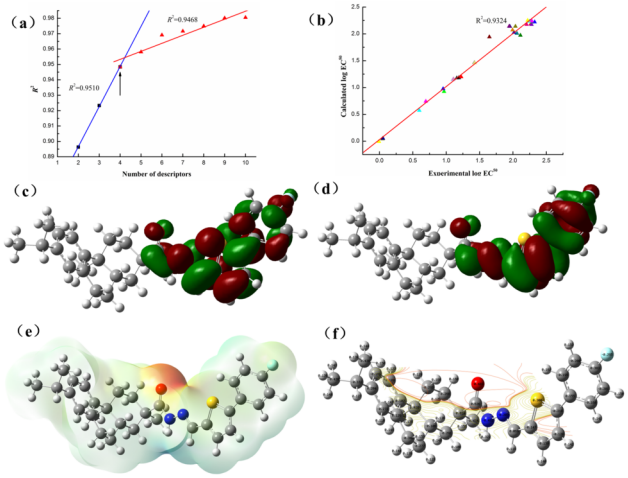

PS_7232_Figure 5.tif

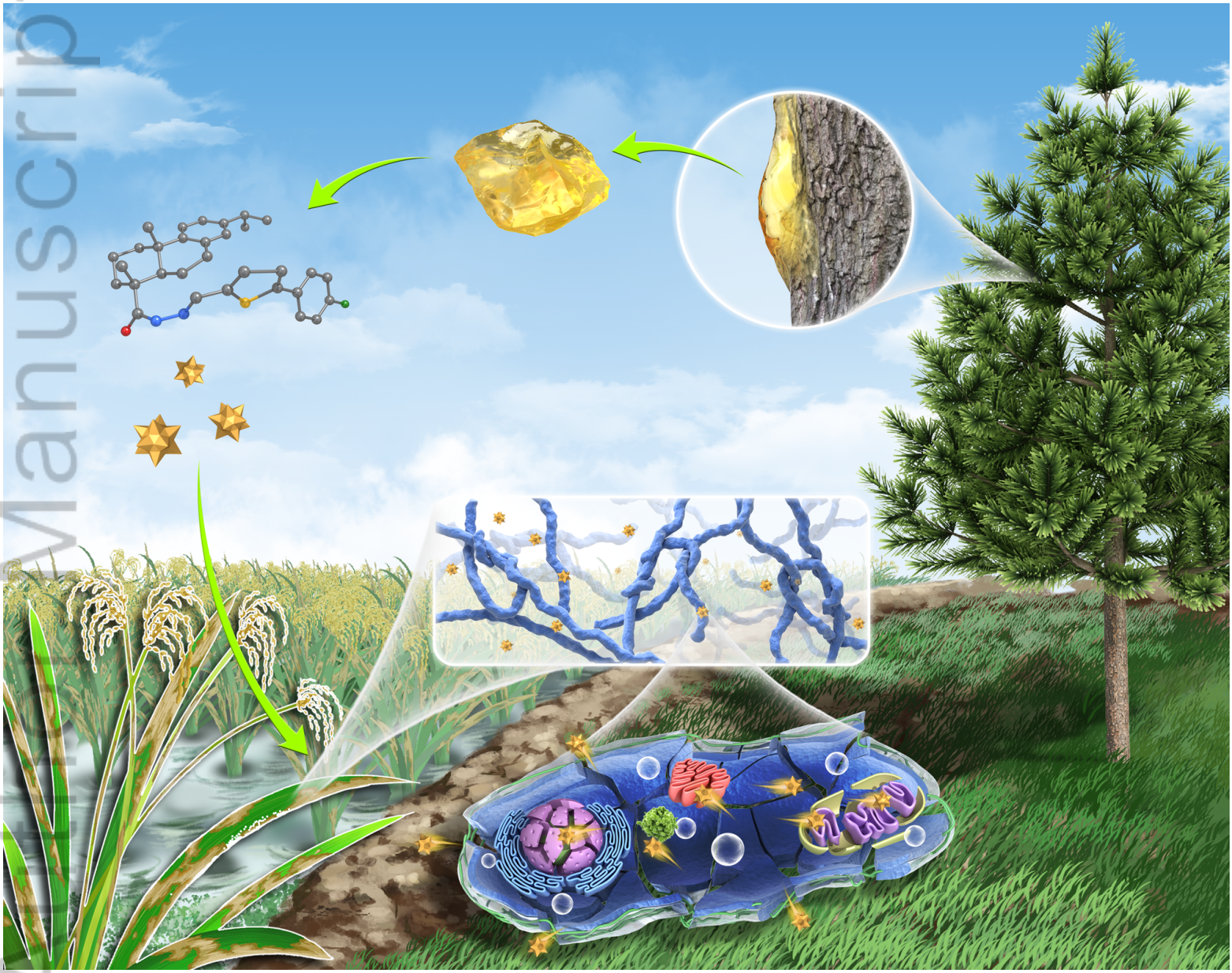

PS_7232_Graphical Abstract Image.tif

Discovery of rosin-based acylhydrazone derivatives as potential antifungal agents against rice *Rhizoctonia solani* for sustainable crop protection

Renle Xu, Shihao Gu, Kun Chen, Jinyu Chen, Yong Wang, Yanqing Gao, Shibin Shang, Zhanqian Song, Jie Song, and Jian Li*

Summary: The rosin-based acylhydrazone fungicides were prepared and their putative modes of action on rice *Rhizoctonia solani* was investigated by physiological and biochemical determination and computational chemistry analysis.

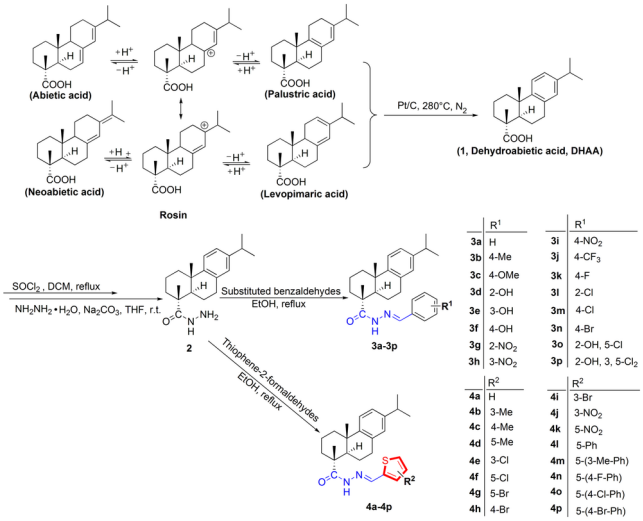

	R^1
3a	H
3b	4-Me
3c	4-OMe
3d	2-OH
3e	3-OH
3f	4-OH
3g	2-NO_2
3h	3-NO_2

	R^1
3i	4-NO_2
3j	4-CF_3
3k	4-F
3l	2-Cl
3m	4-Cl
3n	4-Br
3o	2-OH, 5-Cl
3p	2-OH, 3, 5-Cl_2

	R^2
4a	H
4b	3-Me
4c	4-Me
4d	5-Me
4e	3-Cl
4f	5-Cl
4g	5-Br
4h	4-Br

	R^2
4i	3-Br
4j	3-NO_2
4k	5-NO_2
4l	5-Ph
4m	5-(3-Me-Ph)
4n	5-(4-F-Ph)
4o	5-(4-Cl-Ph)
4p	5-(4-Br-Ph)

PS_7232_Scheme 1.tif